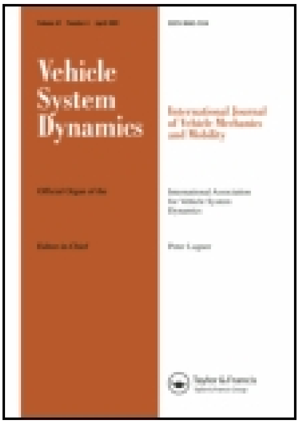

Vehicle System Dynamics: International Journal of Vehicle Mechanics and Mobility
Publication details, including instructions for authors and subscription information:
http://www.tandfonline.com/loi/nvsd20

The stability and mechanical characteristics of heavy haul couplers with restoring bumpstop

Yuan Yao[a], Xu Liu[a], Hongjun Zhang[a] & Shihui Luo[a]
[a] State Key Laboratory of Traction Power, Southwest Jiaotong University, 610031 Chengdu, People's Republic of China
Published online: 24 Oct 2013.

Vehicle System Dynamics, 2014
Vol. 52, No. 1, 26–44, http://dx.doi.org/10.1080/00423114.2013.849352

The stability and mechanical characteristics of heavy haul couplers with restoring bumpstop

Yuan Yao*, Xu Liu, Hongjun Zhang and Shihui Luo

State Key Laboratory of Traction Power, Southwest Jiaotong University, 610031 Chengdu, People's Republic of China

(*Received 15 July 2013; accepted 23 September 2013*)

To investigate the stability and mechanical characteristics of a type of heavy haul coupler with restoring bumpstop, the geometry and force states of couplers were analysed at different yaw angles and the longitudinal forces. The structural characteristics of this coupler were summarised. To aid in the investigation, a multi-body dynamics model with four heavy haul locomotives and three detailed couplers was established to simulate the process of emergency braking. In addition, the coupler yaw instability and lateral forces were tested in order to investigate the effect of relevant parameters on the locomotive's wheelset lateral forces. The results show that only when the bumpstop force exceeds half of the coupler longitudinal compression force, can the follower be rotated and the yaw angle of the coupler increase. The bumpstop preload is the most important stabilising factor. The coupler lateral force is constant when the coupler longitudinal force is smaller than the critical values of 2000, 1400 and 1150 kN at coupler free angles of 7°, 8° and 9°, respectively, for operation on straight track. The coupler free angle and the locomotive's lateral clearance of the secondary stopper are important in decreasing the wheelset lateral forces of the locomotive. It is advised that a smaller locomotive's secondary lateral suspension stiffness, a free clearance of 35 mm and an elastic clearance of 15 mm from the secondary lateral stopper be selected. If the coupler's free angle is less than the self-stabilising angle which is 5.5° for operation on straight track, the coupler is stable no matter how great the longitudinal force is. The wheelset lateral forces are allowed at the coupler longitudinal force of 2500 kN when the free angle is 6°. These studies establish meaningful improvements for the stability of couplers and match the heavy haul locomotive with its suspension parameters.

Keywords: heavy haul coupler; coupler lateral force; bumpstop; locomotive; derailment

1. Introduction

A larger coupler lateral force caused by emergency braking may lead to the derailment of the locomotive located in the middle of a train. A smaller lateral force on a heavy haul coupler is required as the train tonnage and speed increase. The repeated occurrence of train derailment caused by emergency breaking is a clear indication that both production and operation departments as well as academic institutions require a better understanding of how to prevent these accidents.[1–4] Several researchers previously investigated the longitudinal dynamics of a long train, and discussed the effects of buffer parameters on a train's longitudinal impact forces.[5–8] Cole and co-workers [9–11] conducted many studies on the derailment issues involving heavy haul trains. These included longitudinal dynamics, wagon connection

*Corresponding author. Email: yyuan8848@163.com

models, comfort, train management and driving practices. A comprehensive nonlinear model was developed [4,6] to study severe braking conditions and minimise the tendency of train derailment. These studies, however, did not consider the problem of decreased stability when longitudinal compressive forces are applied to a coupler. The current understanding of heavy haul train coupler stability and its effect on derailment is still rudimentary and needs to be studied further.

In China, heavy haul locomotive couplers can currently be divided into two types according to their structure. The first coupler type has an arc contact surface at its end. Wu et al. [12,13] used a rotation joint to simulate the yoke key of this coupler, and postulated that friction torques supplied by two end contact surfaces will stabilise the coupler by balancing the yaw moment caused by the coupler's yaw angle. Yao et al. [14] analysed the yaw stability of arc couplers with the friction circle theory and illustrated the importance of the coupler's arc friction coefficient and the locomotive's lateral suspension stiffness to the bearing capacity of this type of coupler. The second coupler typesets an elastic bumpstop which can prevent a larger yaw angle and provide lateral stability to the coupler. Ma et al. [15] studied the effects of this coupler and buffer system on the dynamic performance of heavy haul locomotives to better understand possible derailment issues during braking. In his study, the bumpstop function was simulated by a simplified nonlinear stiffness. In this paper, the geometric and mechanical characteristics of the second coupler type were investigated by formula calculations and a simulation of locomotive breaking that used a model created based on actual component specifications. The matching principle of the coupler with the secondary suspension parameters of a locomotive was studied for reducing the wheelset lateral forces when the train was braking. These studies have both theoretical and practical engineering value to help improve the bearing capacity of this type of coupler.

2. The structural characteristics of the coupler with restoring bumpstop

2.1. *The coupler structure and force analysis*

A heavy haul locomotive coupler with restoring bumpstop is shown in Figure 1. It is composed of a coupler yoke, rubber buffer, follower, bumpstop, yoke key and coupler. Note that the end of the coupler has a shoulder which is used to limit its yaw angle by contacting the bumpstop. The coupler and the coupler yoke are connected by a round yoke key. When the coupler

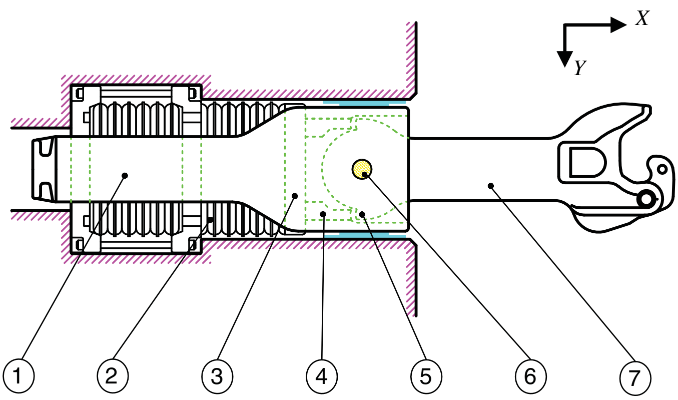

Figure 1. The structure of a coupler with restoring bumpstop. (1) Coupler yoke, (2) Rubber buffer, (3) Follower, (4) Bumpstop, (5) Shoulder, (6) Yoke key and (7) Coupler.

Table 1. Parameter values.

Parameter	Description	Value
l	Half of the coupler length (m)	0.712
b	Lateral distance from bumpstop to yoke key (m)	0.135
c	Half of the width of the coupler yoke (m)	0.150
l_b	Half of the bogie longitudinal distance (m)	5.075
l_c	Half of the longitudinal distance of coupler mounting seats (m)	17.652

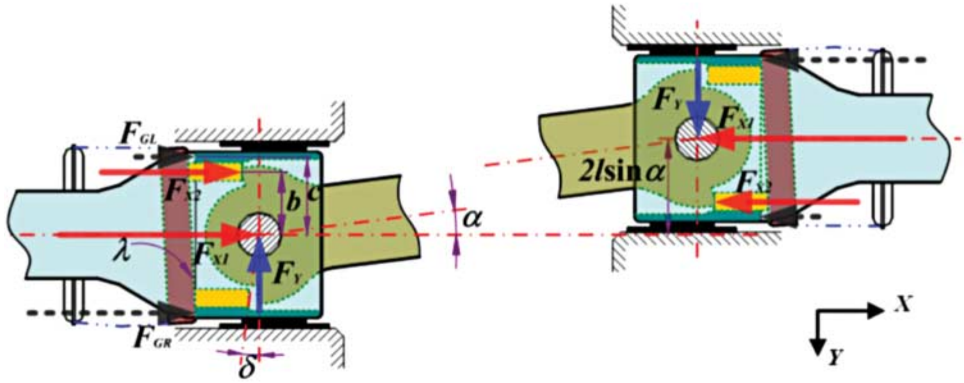

Figure 2. The geometry and force analysis of coupler for operation on straight track.

is pulled, it pulls the yoke key and moves the coupler yoke, thus compressing the rubber buffer and providing both traction stiffness and damping. When the coupler is compressed, it pushes the yoke key and moves the coupler yoke to compress the follower and the buffer. This coupler's main feature is the adoption of bumpstops to prevent the increase in the yaw angle. The coupler's parameter values are shown in Table 1.

When the yaw angle of coupler is less than its free angle, the coupler can be seen as a two-force rod. The coupler rotates under the longitudinal compressive force and is balanced by the locomotive suspension. When the bumpstop is in contact with the shoulder as shown in Figure 2, the yaw moment is greater than the restoring moment caused by the locomotive suspension, and the yaw angle α increases to the free angle δ. At that moment, the end of the coupler experiences the two longitudinal forces F_{X1}, F_{X2} offered by the yoke key and the bumpstop, respectively. These forces can be calculated according to the force equilibrium. In addition, the follower experiences the longitudinal forces F_{GL} and F_{GR} offered by the both sides of the coupler yoke. These are both equal to half of the coupler longitudinal force. Only when the bumpstop force F_{X2} is greater than the longitudinal force F_{GL}, can the follower be rotated, further increasing the coupler's yaw angle. Due to these circumstances, the bumpstop preload is a very important factor for stabilising the coupler. There is a lateral force that occurs when the coupler rotates under the compressive longitudinal force and the coupler's lateral force will increase the wheelset lateral forces of locomotive or even lead to derailment.

2.2. *The geometry and force analysis of coupler for operation on straight track*

According to the relationship between a coupler's yaw angle and its free angle, the geometry and force states of the coupler can be analysed with the following three cases when the locomotive is for operation on straight track:

(1) When the coupler yaw angle α is less than the free angle δ, the coupler can be seen as a two-force rod. The coupler lateral force F_Y and the longitudinal compression force F_{cx} have the following relationship:

$$F_Y = F_{cx} \cdot \tan\alpha. \tag{1}$$

When the locomotive's lateral suspension causes a restoring force larger than the coupler's lateral force, F_Y, the coupler is stable and its yaw angle will not increase. Accordingly, F_{cx} satisfies the following equation

$$F_{cx} \leq k_{cy} l \cos\alpha, \tag{2}$$

where $k_{cy} = (l_b/l_c)^2 k_s$, k_{cy} is the lateral equivalent stiffness of the coupler mounting seat; k_s is the lateral suspension stiffness of a single bogie which is a series stiffness of the primary and secondary suspension; l_b is half of the bogie longitudinal distance of the locomotive; l_c is half of the longitudinal distance of the coupler mounting seats and l is half of the coupler length.

For this study, the longitudinal compressive force must be less than 270 kN to ensure that the bumpstop could not be contacted.

(2) The coupler yaw angle α is equal to the free angle δ within a certain range of F_{cx} when the longitudinal bumpstop forces F_{X2} and F_{cx} satisfy the following equation:

$$F_{X2} < \frac{c}{b+c} F_{cx} \approx 0.5 F_{cx}. \tag{3}$$

At this moment, the coupler lateral force F_Y is proportional both to the yaw angle α and the lateral equivalent stiffness of the coupler mounting seat k_{cy}, while having nothing to do with the longitudinal force F_{cx}

$$F_Y = k_{cy} l \sin\alpha. \tag{4}$$

The force equilibrium equations of coupler are as follows:

$$F_{X1} + F_{X2} = F_{cx}, \tag{5}$$

$$F_{X1} 2l \sin\alpha + F_{X2}(2l\sin\alpha - 2b) - F_Y 2l \cos\alpha = 0. \tag{6}$$

Taking the nonlinear lateral suspension stiffness of the locomotive into account, the bumpstop longitudinal forces at different yaw angles and the coupler longitudinal forces are shown in Figure 3. The follower rotates if the bumpstop force is greater than half of the coupler longitudinal force. The critical coupler forces of 2000, 1400 and 1150 kN will rotate the follower at coupler yaw angles of 7°, 8° and 9°, respectively.

(3) If Equation (3) cannot be satisfied, the coupler yaw angle α is larger than the free angle δ and their relationship is as follows:

$$\alpha = \delta + 2\lambda, \tag{7}$$

where λ is the rotation angle of the follower and it is proportional to the bending stiffness of the rubber buffer and the bumpstop force. When the coupler longitudinal force increases, so too does the follower rotation angle and the coupler lateral force. It is needed to overcome the longitudinal preload of the bumpstop (about half of the coupler longitudinal force) and the restoring torque caused by the bending stiffness of the rubber buffer that the follower can be rotated, which is advantageous to stabilise the coupler. At this moment, the coupler can be

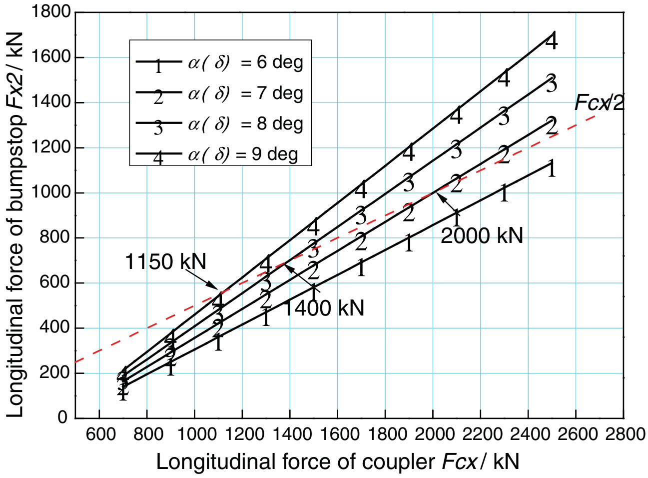

Figure 3. The longitudinal forces of the coupler and the bumpstop.

equivalent to a single-rod model with rotary stiffness at both of its ends with a force balance equations of

$$F_{cx}2l\sin\alpha - F_{cx}b - k_{rot}(\alpha - \delta) - F_Y 2l\cos\alpha = 0, \tag{8}$$

where k_{rot} is the bending stiffness of the rubber buffer.

In Equation (8), the first term is the coupler yaw torque, the second term is the restoring torque caused by bumpstop preload, the third term is the restoring torque caused by the buffer and the final term is the restoring torque caused by lateral suspension of the locomotive. If the coupler yaw angle α satisfies Equation (9), the sum of the first and the second terms equals 0, and α is called the self-stabilising angle. Simply put, if the free angle of the coupler is smaller than or equal to the self-stabilising angle, the coupler will be stable no matter how great the longitudinal force is. In this study, the self-stabilising angle of the couplers used is 5.5° for operation on straight track:

$$\alpha = \sin^{-1}\left(\frac{b}{2l}\right). \tag{9}$$

The nonlinear static compressive stiffness of the rubber buffer is shown in Figure 4. As shown in Figure 5, the coupler equilibrium yaw angle at different longitudinal forces and the free angles can be calculated according to Equation (8). When the longitudinal force is greater than the critical coupler force, the equilibrium angle and the lateral force of the coupler increase with the longitudinal force. The maximum coupler yaw angle of 11.3° is dependent on the lateral clearance of the secondary stopper and the length of the coupler, where there are 50 and 1424 mm, respectively.

2.3. *The geometry and force analysis of coupler in curves*

When the locomotive passes the curves, there is a yaw angle between the coupler and the front or rear car body, both of which will be increased by the coupler longitudinal compressive force, as shown in Figure 6. The small angles of η_1 and η_2 are the yaw angles of the front and rear car body which can be ignored in the geometry analysis of the coupler. β is the coupler yaw angle caused by the curve. α is the yaw angle caused by the coupler longitudinal compressive

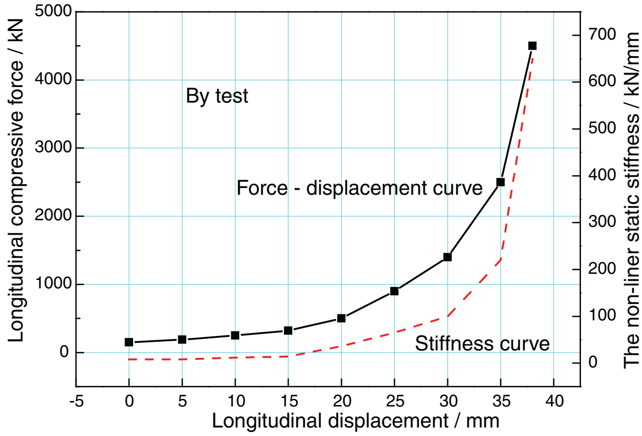

Figure 4. The nonlinear static compressive stiffness of the rubber buffer.

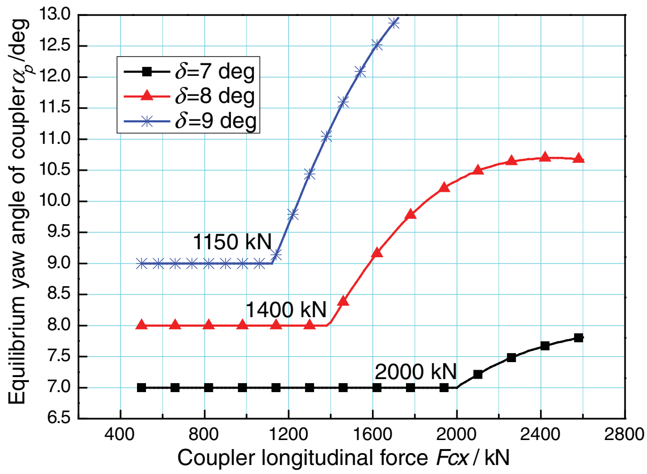

Figure 5. The coupler equilibrium yaw angle at different longitudinal forces and the free angles.

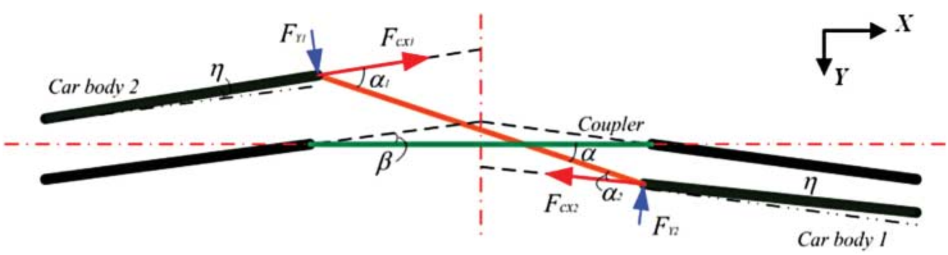

Figure 6. The yaw angle of coupler in curves.

force and α_1 and α_2 are the yaw angles of the coupler relative to the rear and front car body, respectively. The angles of α_1, α_2, β and α have the following relationship:

$$
\begin{aligned}
\alpha_1 &= \alpha + \beta, \\
\alpha_2 &= \alpha - \beta.
\end{aligned}
\tag{10}
$$

It is equivalent to

$$\alpha_1 = \alpha_2 + 2\beta, \qquad \alpha = \tfrac{1}{2}(\alpha_1 + \alpha_2). \tag{11}$$

The angle β is dependent on the longitudinal distance of the coupler mounting seat $2l_c$, the length of coupler $2l$ and the curve radius R:

$$\beta \approx \sin^{-1}\left(\frac{l_c + l}{R}\right). \tag{12}$$

In this study, when R is 300, 800 and 1600 m, β is 1.8°, 0.68° and 0.34°, respectively. Since β is positive, the yaw angle α_1 relative to the rear car body is greater than α_2 relative to the front car body. This will cause the coupler angles to increase under the compressive force. The leading coupler on the rear vehicle will rotate towards the direction of the curve (i.e. low rail). This is more evident on curves of small or medium radii.

According to the relationship between the yaw angles at both ends of the coupler with the coupler free angle, the geometry and force states of couplers in curves can be categorised with the following four cases:

(1) $\delta > \alpha_1 > \alpha_2$

The coupler is a two-force rod and the compound forces can be calculated as following the assumption of small angles:

$$F_{cx1} \approx F_{cx2}, \tag{13}$$

and

$$\frac{F_{Y1}}{F_Y 2} = \frac{F_c \sin\alpha_1}{F_c \sin\alpha_2} \approx \frac{\alpha_1}{\alpha_2} = \frac{\alpha + \beta}{\alpha - \beta}. \tag{14}$$

The lateral force at the rear end of the coupler is larger than that at the front end. This means that the wheelset lateral forces on the front bogie caused by braking are greater than those on the rear bogie in a same locomotive located in the middle of a train. This is more evident on curves of small or medium radii.

In order to balance or stabilise a coupler under a huge compressive force, the sum of the coupler lateral forces at the two ends must be less than or equal to the restoring force caused by the locomotive's lateral suspension:

$$F_{Y1} + F_{Y2} = F_{cx} \cdot (\sin\alpha_1 + \sin\alpha_2) \le k_{cy} \cdot 2l \sin a. \tag{15}$$

It is the same as the analysis in the straight line that the longitudinal compressive force of coupler must be less than 270 kN to ensure that the coupler yaw angle is smaller than the free angle.

(2) $\alpha_1 = \delta, \alpha_2 = \delta$

In this case, the bumpstop is in contact with the shoulder at the rear end of the coupler and the yaw angle of this end is equal to the free angle. The coupler yaw angle relative to the front car body, however, is less than the free angle. Since the rear end experiences two longitudinal forces of F_{X11} and F_{X12}, the coupler is not a two-force rod. According to the principle of moment equilibrium, the two forces of F_{X11} and F_{X12} are equivalent to a force $F_{cx1}(= F_{X11} + F_{X12})$ in the same direction, where the distance to the yoke key is a.

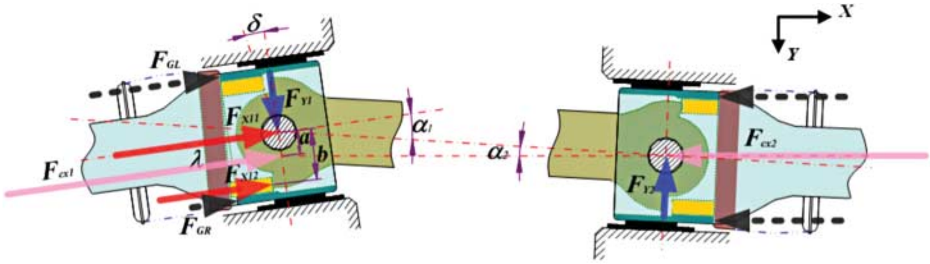

Figure 7. The force state of the coupler with one end contact.

Table 2. The coupler forces in the critical deflection state of the rear follower.

$\alpha_1 = \delta, \alpha_2 = \delta$	Longitudinal force (kN)			Lateral force at the rear end (kN)		
δ	R300	R800	R1600	R300	R800	R1600
5	1682	685	609	67.1	27.3	24.3
6	719	550	538	41.2	31.5	30.8
7	555	521	514	41.5	38.9	38.4
8	523	500	500	48.2	46.5	46.1

The distance a is related to the ratio of the two forces and its maximum value is the width of shoulder b. Figure 7 shows the force states of the coupler with one end contact:

$$a = \frac{F_{\mathrm{X12}}}{F_{\mathrm{X11}} + F_{\mathrm{X12}}} b. \tag{16}$$

The points of action F_{cx1} and F_{cx2} at the both ends of the coupler form a line to transfer the coupler force which is called as force line. The yaw angles of the force line relative to the car body at the two ends are $\alpha_{1\mathrm{e}}$ and $\alpha_{2\mathrm{e}}$, respectively, which can be obtained by the following equation on the assumption of small angles:

$$\alpha_{i\mathrm{e}} \approx \alpha_i - \tan^{-1}\left(\frac{a}{2l}\right), \quad i = 1, 2. \tag{17}$$

With the increase in the longitudinal force and yaw angle of coupler, the bumpstop force F_{X12} increases and the longitudinal force of the yoke key F_{X11} decreases. If F_{X12} equals F_{X11}, the follower is in a critical rotated state in which a is equal to half of b. So, the critical coupler longitudinal forces needed to rotate the follower at different free angles can be calculated by the following equation on the condition that a equals half of b:

$$F_{\mathrm{cx}}(\sin\alpha_{1\mathrm{e}} + \sin\alpha_{1\mathrm{e}}) - k_{\mathrm{cy}} 2l \sin\alpha = 0. \tag{18}$$

Due the assumption of small yaw angles, this equation can be simplified as

$$F_{\mathrm{cx}}\left(2\alpha_1 - 2\beta - \frac{b}{2l}\right) - 2k_{\mathrm{cy}} l(\alpha_1 - \beta) = 0. \tag{19}$$

Table 2 shows the coupler forces in the critical rotated state of the follower. With the increase in the free angle, the allowed coupler longitudinal force decreases and the undesirable lateral force increases in curves. The bigger the curve radius is, the smaller the allowed coupler longitudinal force will be.

Based on Equation (19), if the coupler free angle is smaller than $\beta + b/4l$, the yaw angle of the coupler cannot be increased no matter how great the longitudinal force is.

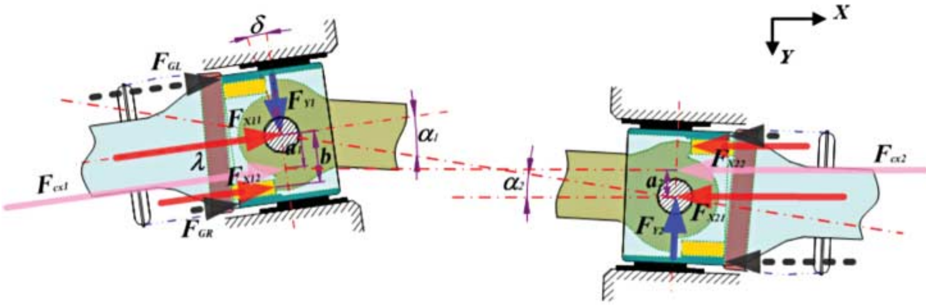

Figure 8. The force states of coupler with the contact of both ends.

(3) $\alpha_1 > \delta, \alpha_2 = \delta$

In this case, the bumpstops are in contact with the shoulder at both ends of the coupler and the yaw angle of the front end is equal to the free angle. The yaw angle of the coupler relative to the rear car body, however, is larger than the free angle. According to the principle of moment equilibrium, the two longitudinal forces F_{X21} and F_{X22} are equivalent to the force $F_{cx2}(= F_{X21} + F_{X22})$ in the same direction as shown in Figure 8.

When the distance of the point from the action F_{cx2} to the yoke key in the front end equals $0.5b$, the front follower is in the critical rotated state. Additionally, the bumpstop force F_{X12} is greater than F_{X11} in the rear end and the rotated angle of the follower in the rear end equals β. The distance a_1 can be calculated using the following equation:

$$a_1 = \frac{b}{2} + \frac{k_{\mathrm{rot}}\beta}{2F_{\mathrm{cx1}}}. \tag{20}$$

The yaw angles of the force line relative to the two car bodies are $\alpha_{1\mathrm{e}}$ and $\alpha_{2\mathrm{e}}$, respectively, which can be obtained by the following equation on the assumption of small yaw angles:

$$\alpha_{i\mathrm{e}} \approx \alpha_i - \tan^{-1}\left(\frac{a_1 + a_2}{2l}\right) = \alpha_i - \tan^{-1}\left(\frac{b}{2l} + \frac{k_{\mathrm{rot}}\beta}{4lF_{\mathrm{cx1}}}\right), \quad i = 1, 2. \tag{21}$$

The critical forces needed to rotate the front follower at different free angles can be calculated by the following equation on the condition that a_2 equals half of b:

$$2F_{\mathrm{cx}}\left(\alpha_2 + \beta - \frac{b}{2l} - \frac{k_{\mathrm{rot}}\beta}{4lF_{\mathrm{cx1}}}\right) - k_{\mathrm{cy}}2l\sin\alpha = 0. \tag{22}$$

Table 3 shows the coupler forces in the critical rotated state of the front follower. With the increase in the coupler free angle, the allowed coupler longitudinal force decreases and the undesirable lateral force increases in curves. The bigger the curve radius is, the larger the allowed coupler longitudinal force will be at a small free angle of 5–6°. However, the rule is opposite at a larger free angle of 7–8°.

Based on Equation (22), if the free angle of a coupler is smaller than $-\beta + b/2l$, the coupler has a self-stabilising characteristic.

(4) $\alpha_1 > \delta, \alpha_2 > \delta$

In this case, the bumpstops are in contact with the shoulder at both ends of the coupler and the yaw angles at the two ends are greater than the free angle. According to the principle of moment equilibrium, the forces at both ends can be simplified and the formed

Table 3. The coupler forces in the critical deflection state of the front follower.

$\alpha_1 = \delta, \alpha_2 = \delta$	Longitudinal force (kN)			Lateral force at the rear end (kN)		
δ	R300	R800	R1600	R300	R800	R1600
5	2985	9452	∞	131	142	41.6
6	1912	2236	2492	104	62.7	48.4
7	1476	1439	1419	98.7	60.8	49.5
8	1239	1132	1084	98.9	64.8	55.1

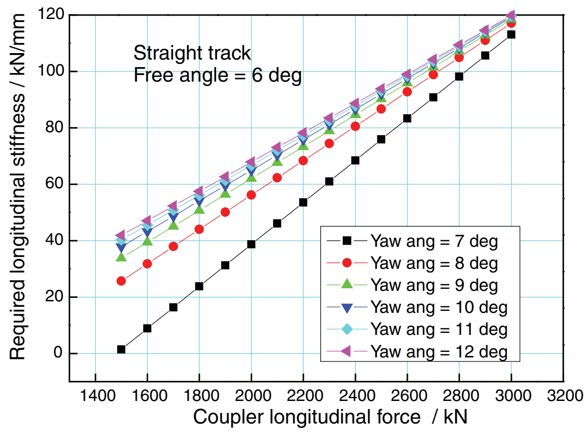

Figure 9. The required longitudinal stiffness of buffer for the coupler stability.

force line can be seen as a two-force rod. The force equilibrium equation is as follows:

$$2F_{\rm cx}\left(\alpha_2 + \beta - \frac{b}{2l} - \frac{k_{\rm rot}(\alpha_2 + \beta - \delta)}{4lF_{\rm cx}}\right) - k_{\rm cy}2l\sin\alpha = 0. \tag{23}$$

Only when the bending stiffness of the rubber buffer in Equation (23) is satisfied can the coupler be stabilised. According to the relationship between the bending and longitudinal stiffness of the rubber buffer as shown in Equation (24), the required longitudinal stiffness of the buffer needed to stabilise the coupler at different longitudinal forces is shown in Figure 9. When the coupler longitudinal force reaches 3000 kN, the longitudinal stiffness of the rubber buffer should be greater than 100 kN/mm:

$$k_{\rm rot} \geq \frac{4l}{\alpha_2 + \beta - \delta}\left(F_{\rm cx}\left(\alpha_2 + \beta - \frac{b}{2l}\right) - k_{\rm cy}l(\alpha_2 + \beta)\right), \tag{24}$$

$$k_{\rm rot} = \frac{8c^2}{3}k_{\rm bx}. \tag{25}$$

2.4. *Summary*

(1) This type of coupler adopts the use of bumpstops to prevent the yaw angle increase when a train is braking. When the coupler longitudinal force is greater than 270 kN in this study, the lateral coupler force component cannot be balanced by the locomotive lateral suspension and the yaw angle increases to the free angle allowed by the bumpstop. The bumpstop force increases with the increase in the longitudinal force and the yaw angle of coupler.

Only when the bumpstop force exceeds half of the coupler longitudinal compressive force can the follower be rotated and the coupler yaw angle further increases. The bumpstop preload is the most important stabilising factor and the free angle significantly affects the stability.

(2) A larger coupler longitudinal force can lead to the derailment of a locomotive. This usually occurs when the train is emergency braking for operation on straight track. Therefore, there is more concern about the performance of couplers for operation on straight track. The self-stabilising angle of the coupler is 5.5° for operation on straight track, meaning the coupler will stabilise itself no matter how great the longitudinal force may be. If the free angle is greater than the self-stabilising angle, however, this important feature is lost.

(3) When the coupler longitudinal force is less than a certain value, the follower cannot be rotated and the coupler yaw angle is equal to the free angle. At this moment, the coupler lateral force is constant, and it has nothing to do with the coupler longitudinal force for operation on straight track. Both a smaller lateral suspension stiffness and a smaller free angle will help reduce the coupler lateral force. The critical values of 2000, 1400 and 1150 kN will rotate the follower at the coupler free angles of 7°, 8° and 9°, respectively. If the coupler longitudinal force is greater than these values, the yaw angle and the coupler lateral force increase with the coupler longitudinal force.

(4) When the yaw angle is smaller than the free angle, a larger lateral suspension stiffness of a locomotive tends to reduce the yaw angle and the lateral force of coupler. The action of the bumpstop, however, is a more prevalent occurrence, so a small lateral suspension stiffness should be selected to reduce the coupler lateral force. The selection of an appropriate lateral clearance of the locomotive's secondary stopper is of importance that the too small one lead to an increase in the lateral equivalent stiffness of locomotive suspension, and the too larger one lead to an increase in the yaw angle of coupler. All of them cause a larger coupler lateral force, something that should be avoided in engineering.

(5) The restoring stiffness supplied by the bumpstop is equivalent to the offset of the act point of the coupler force which reduces the yaw angle of the force line for decreasing the coupler lateral force. The lateral force at the rear end is larger than that at the front end when the locomotive passes the curves and the coupler lateral force increases with the

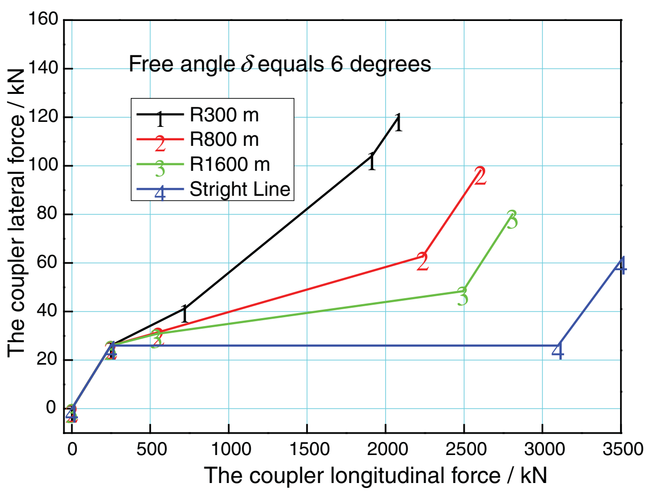

Figure 10. The coupler lateral force at different tracks.

decrease in curve radius. As shown in Figure 10, the coupler lateral force increases with the longitudinal force in curves. However, the lateral force is a constant within a range of the longitudinal force for operation on straight track.

3. Multi-locomotive dynamic simulation model

In order to verify the theoretical analysis and accurately find the relationship between a coupler's bearing capacity and a locomotive's secondary suspension parameters, the multi-body dynamics software, SIMPACK, was used to build the locomotive and the detailed coupler model. The simple train model which is composed of four locomotives can simulate the processes of emergency braking and lateral coupler over turning forces with appropriate boundary conditions. The main impact factors of the coupler's bearing capacity and the effect of the suspension parameters of the locomotive on the wheelset lateral forces had been analysed.

3.1. *The locomotive dynamics model*

This locomotive model was established according to an actual heavy haul locomotive in China, as shown in Table 4. The model consists of four locomotives and three couplers as shown in Figure 11. The longitudinal forces F1 and F2 are applied to both ends of the locomotives separately and the braking torques are applied to each wheelset to simulate the longitudinal impulse caused by emergency braking. These studies focus on the middle two locomotives.

Table 4. The main parameters of locomotive.

Axle arrangement	Axle load (T)	Wheel base (m)	Bogie distance (m)	Coupler seats distance (m)
$2B_0$	27	2.6	10.15	17.652
Axle guidance stiffness (signal axlebox) (kN.mm^{-1})			Secondary suspension stiffness (one side in a bogie) (kN.mm^{-1})	
Longitudinal	Lateral	Vertical	Lateral	Vertical
162.6	4.06	1.317	0.58	14

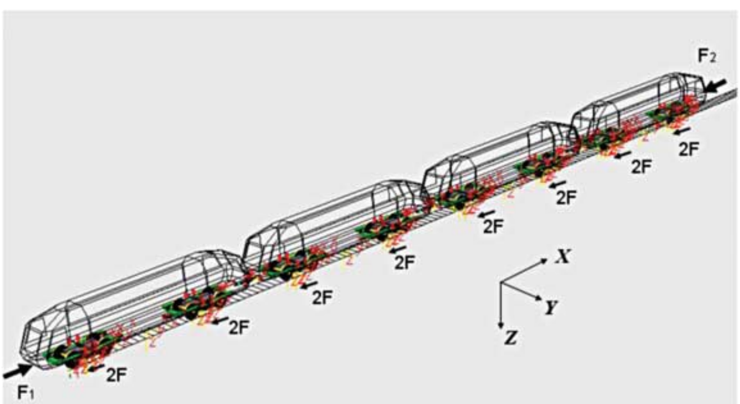

Figure 11. The simple train model composed of four locomotives and three couplers.

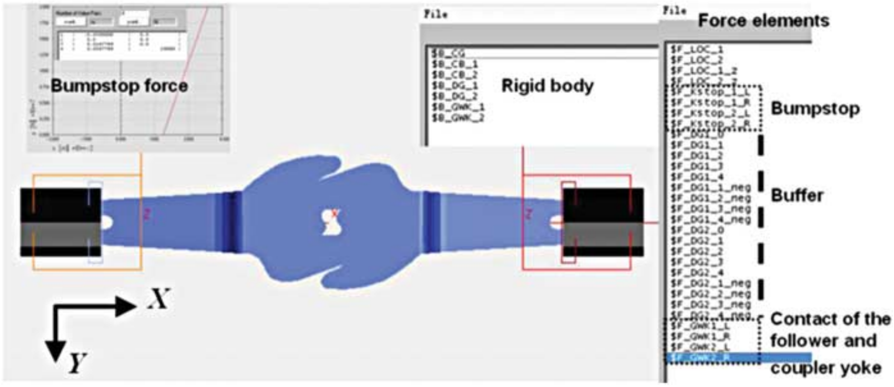

Figure 12. The coupler dynamics model including 7 rigid bodies and 30 force elements.

3.2. *The coupler dynamics model*

According to the structure and size of the actual coupler, the multi-body dynamics model of the coupler including 7 rigid bodies and 30 force elements is shown in Figure 12. The follower has the freedom to yaw and move longitudinally. The coupler yoke has the freedom to move longitudinally while the coupler can move longitudinally, pitch and yaw. The nonlinear longitudinal stiffness of the buffer is shown in Figure 5 and nine component spring elements are arranged discretely in the transverse direction to simulate the bending stiffness of the buffer. The bumpstop is modelled by a nonlinear unilateral contact force element with clearance. Similarly, the contact between the follower and coupler yoke is modelled by the unilateral contact force element.

3.3. *The boundary conditions and calculation conditions*

To simulate the locomotives located in the middle of a 20,000 ton heavy haul train for operation on straight track, the following boundary conditions were applied. The maximum coupler longitudinal force was set at 2500 kN. The initial speed before breaking was 80 km/h. And lastly, the braking force for a single locomotive was set as 255 kN. The track irregularity of AAR5 [16] is used. The coupler force curve in the time domain is shown in Figure 13.

4. The simulation results of the locomotive dynamics

4.1. *The wheelset lateral forces in the straight line*

Larger coupler longitudinal forces which can lead to the derailment of locomotives usually occur when a train is emergency braking for operation on straight track. This braking scenario has been known to cause several derailment accidents. Therefore, there is more concern about the performance of couplers for operation on straight track. According to the dynamics model and the boundary conditions in Section 3, the wheelset lateral forces of locomotives were simulated at different longitudinal forces and the coupler yaw angles. Figures 13 and 14 show the coupler yaw angles and the wheelset lateral forces of locomotives at different longitudinal forces. In these cases, the lateral clearance of the locomotive's secondary stopper is composed of the free clearance of 35 mm and the elastic clearance of 15 mm. When the coupler cannot be stabilised by the locomotive's lateral suspension, the coupler yaw angle suddenly increases

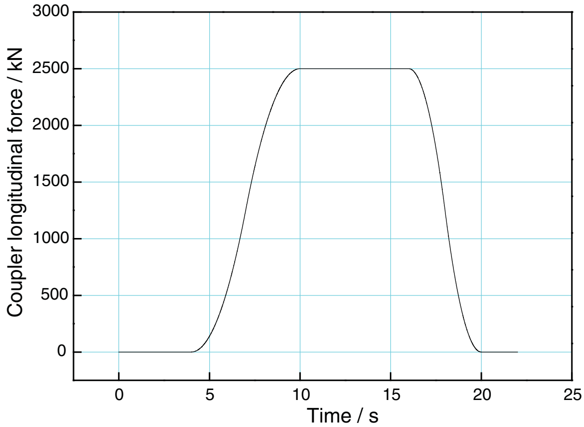

Figure 13. The coupler longitudinal force curve in the time domain.

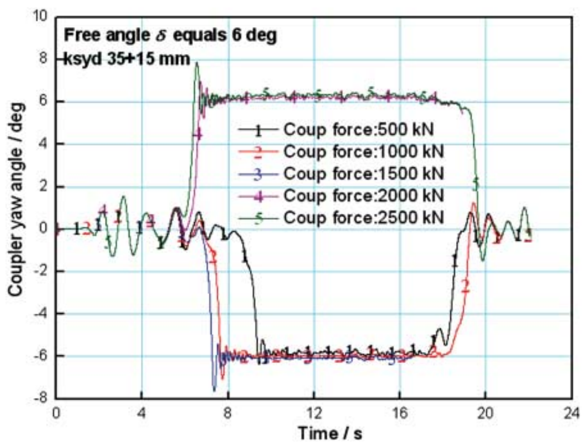

Figure 14. The coupler yaw angles at different longitudinal forces in the time domain.

to the free angle. In severe cases, there is a distinct impact on the follower and a moment on the coupler. As shown in Figure 15, the maximum wheelset lateral forces occur at the moment of coupler overturning due to the overshoot of the yaw angle. Meanwhile, the rim–rail contact caused by the larger lateral force reduces the dynamic wheelset lateral force, which is even less than the wheelset lateral force when the coupler force decreases. The lateral force of the rear wheelset is larger than that on the front wheelset in the same bogie for operation on straight track.

Figure 15 verifies the theoretical analysis in Section 2.2, in which the wheelset lateral force is a constant and has nothing to do with the coupler longitudinal force at a small free angle. The wheelset lateral forces increase with the free angle at the same coupler longitudinal force. Once the follower rotates under a sufficient free angle and coupler longitudinal force, the wheelset lateral forces increase as well. When the coupler free angle is less than 6°, the wheelset lateral forces of the locomotive under the maximal coupler longitudinal force of 2500 kN are less than the allowable value of 98.3 kN calculated with the British standard of EN 14363 (Figure 16). However, the wheelset lateral forces cannot meet the required maximal coupler force once the free angle is larger than 7°.

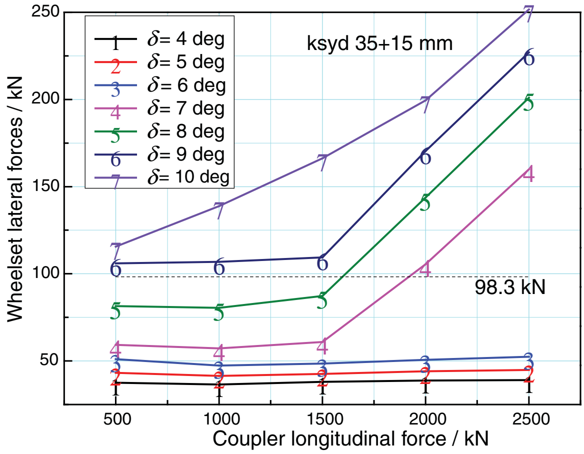

Figure 15. The wheelset lateral at different longitudinal forces and yaw angles.

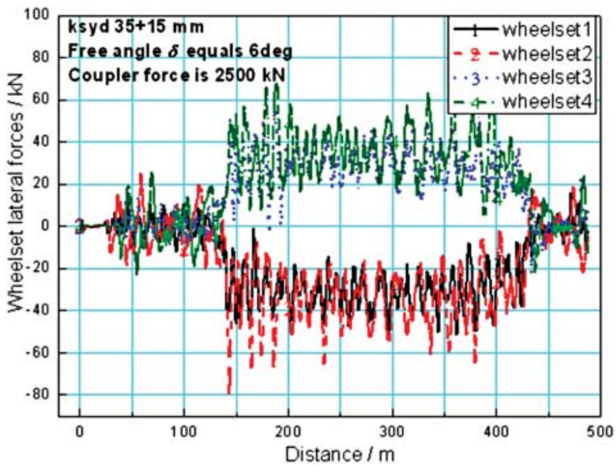

Figure 16. The wheelset lateral forces in the time domain at the free angle of 6°.

Table 5. The curve settings of the simulation.

Conditions	Radius (m)	Transition curve (m)	Circle curve (m)	Cant (mm)	Speed (km/h)
1	300	80	300	120	60
2	800	120	400	130	80
3	1600	160	600	100	80

4.2. *The wheelset lateral forces in curves*

According to the force analysis of couplers in curves, there is an initial coupler yaw angle before train braking which will lead to greater coupler lateral force. This is especially true in tight curves. In order to verify the theoretical analysis and accurately calculate the wheelset lateral forces of locomotives in curves, the dynamics model was simulated with curves of different radii as shown in Table 5.

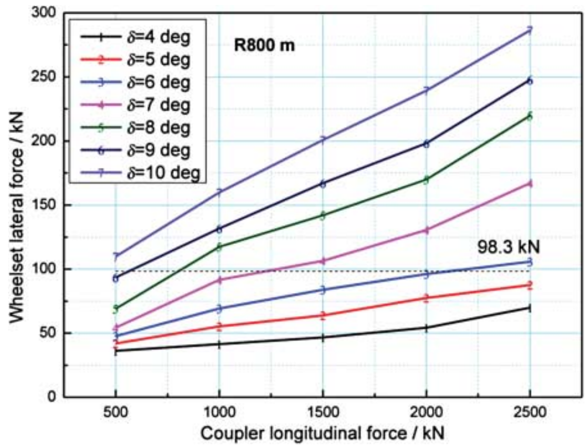

Figure 17. The wheelset lateral forces in the curve of R800 m.

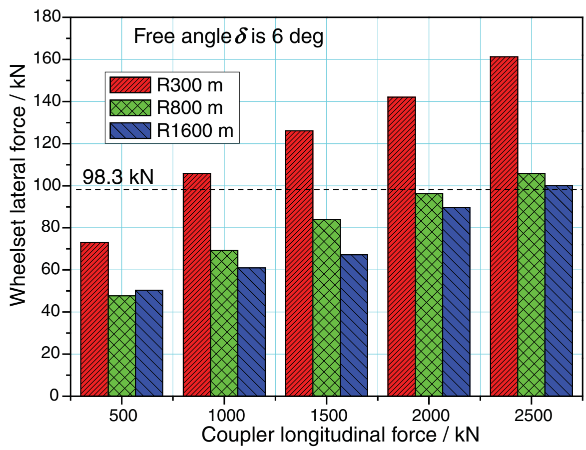

Figure 18. The wheelset lateral forces at the coupler free angle of 6°.

Figures 17 and 18 are the calculated wheelset lateral forces of locomotives in curves under different longitudinal forces and coupler yaw angles. The results indicate the following:

(1) The wheelset lateral force increases with the increase in the coupler longitudinal force especially in curves of medium or small radii.
(2) Reducing the free angle of the coupler will help decrease the wheelset lateral forces.
(3) The leading coupler of the rear vehicle will rotate towards the direction of a curve (i.e. low rail) when the coupler is under a compressive force especially in curves of small or medium radii. This means that the wheelset lateral forces of the front bogie caused by the train braking are greater than that those at the rear bogie located in the middle of the train.
(4) When the coupler free angle is 6°, the maximum allowable coupler longitudinal forces are 900, 2000 and 2400 kN in the curves of R300, R800 and R1600 m, respectively. The allowable longitudinal forces are 700, 1200 and 1800 kN in the curves of R300, R800 and R1600 m, respectively, at the coupler free angle of 7°.

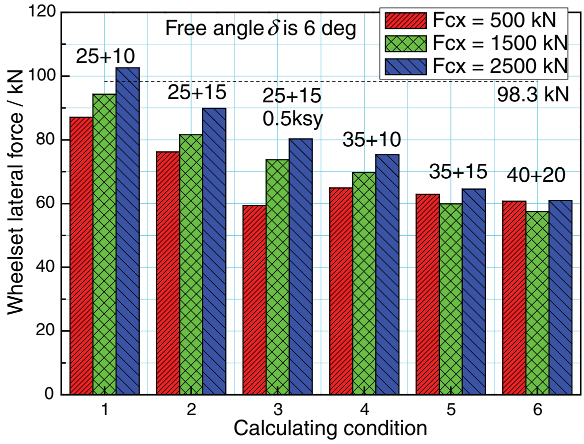

Figure 19. The wheelset lateral forces with different suspension parameters at the free angle of 6°.

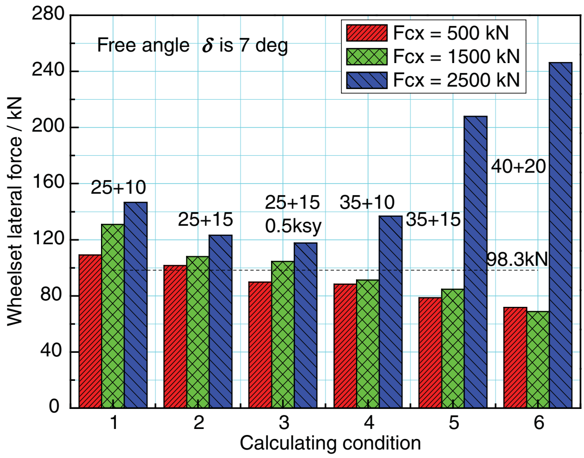

Figure 20. The wheelset lateral forces with different suspension parameters at the free angle of 7°.

4.3. *The effect of the suspension parameters on the wheelset lateral forces*

In order to analyse the influence of secondary suspension parameters on wheelset lateral forces, the dynamics model was simulated with different secondary suspension parameters and coupler yaw angles for operation on straight track. The results about the wheelset lateral force are shown in Figures 19–21 at yaw angle of 6°, 7° and 8°, respectively. The number above the histogram represents the free lateral clearance and the elastic lateral clearance of the locomotive's secondary stopper. The results show that the wheelset lateral force decreases with the increase in lateral clearance of the secondary stopper at the maximum coupler longitudinal force of 2500 kN when the coupler free angle is 6°. However, a larger stopper clearance increases the wheelset lateral force but reversing this trend at a larger longitudinal force once the coupler free angle is more than 6°. In addition, a smaller secondary lateral stiffness tends to reduce the wheelset lateral forces. It is advised that a smaller secondary lateral stiffness as well as a secondary stopper free clearance of 35 mm and elastic clearance of 15 mm be selected so as to reduce the wheelset lateral force. The maximum value of 64.5 kN is reduced by 16% compared to the initial parameters of 25 and 15 mm at the coupler longitudinal force of

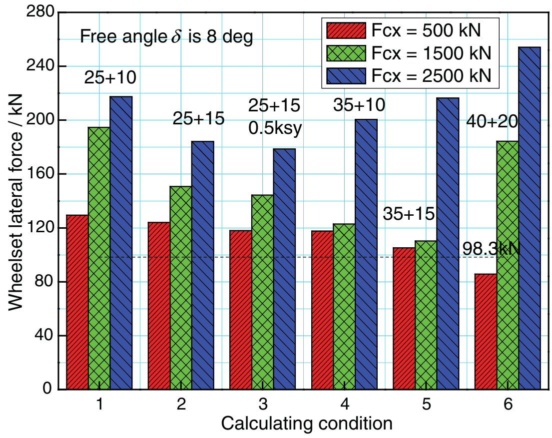

Figure 21. The wheelset lateral forces with different suspension parameters at the free angle of 8°.

2500 kN. If the free angle is equal to 7°, the wheelset lateral forces do not meet the requirement at the maximum longitudinal force of 2500 kN no matter how many the lateral clearance of the secondary stopper is.

5. Conclusions

(1) This type of draft gear assembly adopts the use of bumpstops to prevent the yaw angle increase when a train is braking. In this study, when the coupler longitudinal force was greater than 270 kN, the coupler could not be balanced by the locomotive lateral suspension and its yaw angle increases to the free angle where the bumpstop works. The bumpstop force increases with the increase in the longitudinal force and the coupler yaw angle. Only when the bumpstop force exceeds half of the coupler longitudinal compressive force can the follower be rotated and the coupler yaw angle increase. The bumpstop preload equalling half of the coupler longitudinal force as well as the coupler free angle are the two most important stabilising factors of the coupler.

(2) When the coupler force is less than a certain value, the follower does not rotate and the coupler yaw angle is equal to the free angle. At this moment, the coupler lateral component force is constant and has nothing to do with the coupler longitudinal force. The critical values of 2000, 1400 and 1150 kN will move the follower at the coupler free angles of 7°, 8° and 9°, respectively, for operation on straight track. If the coupler longitudinal force surpasses any of these values, the yaw angle and the coupler lateral force will increase with the increase in the longitudinal force.

(3) A careful selection of the lateral clearance of the locomotive's secondary stopper is important. If it is too small, the lateral equivalent stiffness of a locomotive will increase. If it is too large, the coupler yaw angle will increase. Both of these outcomes cause a larger coupler lateral force which should be avoided in engineering. It is advised that a smaller secondary lateral stiffness as well as the secondary stopper's lateral free clearance of 35 mm and elastic clearance of 15 mm be selected.

(4) A larger coupler longitudinal force can lead to the derailment of a locomotive. This usually occurs when the train is emergency breaking for operation on straight track. Therefore, there is more concern about the performance of couplers for operation on straight track. The self-stabilising angle of coupler is 5.5° for operation on straight track, which means

the coupler will stabilise itself no matter how great the longitudinal force may be. The increase in shoulder width and decrease in coupler length are conducive to an increase in the self-stabilising angle. However, the simulation results show that the wheelset lateral force can be met at the coupler longitudinal compressive force of 2500 kN when the free angle is 6°.

(5) The wheelset lateral force increases with the increase in the coupler longitudinal force in curves. The leading coupler of the rear vehicle will rotate towards the direction of a curve (i.e. low rail) when the coupler is under a compressive force. This is more evident on curves of small or medium radii. This means that the wheelset lateral forces of the front bogie caused by train braking are greater than those of the rear bogie located in the middle of the train. When the coupler free angle is 6°, the maximum allowable coupler longitudinal forces are 900, 2000 and 2400 kN in the curves of R300, R800 and R1600 m, respectively.

Acknowledgement

The authors wish to acknowledge the support of the National Natural Science Foundation of China (No. 51205324), the Fundamental Research Funds for the Central Universities (No. SWJTU11BR050) and Independent Research and Development Project of Key Laboratory (No. 2011TPL_T04).

References

[1] European Institute for Railway Research. Etude del probabilities de derailment de trains de marchandises sous l'influence d'efforts longitudinaux de compression eleves; 1999 (ERRI B177.5/RP1).
[2] Transportation Safety Board of Canada. Railway investigation report R02C0050. Ottawa: Transportation Safety Board of Canada, 2002. Derailment, Canadian National Train Number A-442-51-08 Mile 52.1.
[3] Belforte P, Cheli F, Diana G. Numerical and experimental approach for the evaluation of severe longitudinal dynamics of heavy freight trains. Veh Syst Dyn. 2008;46:937–955.
[4] Durali M, Shadmehri B. Nonlinear analysis of train derailment in severe braking. J Dyn Syst Meas Control. 2003;125: 48–53.
[5] Geike T. Understanding high coupler forces at metro vehicles. Veh Syst Dyn. 2007;45:389–396.
[6] Pugi L, Rindi A, Ercole AG, Palazzolo A, Auciello A. Preliminary studies concerning the application of different braking arrangements on Italian freight trains. Veh Syst Dyn. 2011;49:1339–1365.
[7] Pugi L, Fioravanti D, Rindi A. Modeling the longitudinal dynamics of long freight trains during the braking phase. 12th IFTOMMWorld Congress, Besancon; 2007 June. p. 1–6.
[8] Geike T. Understanding high coupler forces at metro vehicles. Veh Syst Dyn. 2007;45:389–396.
[9] Cole C, Mitchell M, Dudley R, Gerhard L, Fanus V, Ted M. Heavy haul coal train dynamics simulation comparisons of the COALlink and central Queensland systems. Proceedings of the 7th international heavy haul conference, Brisbane, Australia; 2001. p. 217–223.
[10] Simson SA, Cole C. Simulation of curving at low speed under high traction for passive steering hauling locomotives. Veh Syst Dyn. 2008;46:1107–1121.
[11] Cole C, Sun YQ. Simulated comparisons of wagon coupler systems in heavy haul trains. Proc IMechE F: J Rail Rapid Transit. 2006;220:247–256.
[12] Wu Q, Luo SH, Xu ZQ, Ma WH. Coupler jackknifing and derailments of locomotives on tangent track. Veh Syst Dyn. 2013;51(11):1784–1800.
[13] Wu Q, Luo SH, Wei CF, Ma WH. Dynamics simulation models of coupler systems for freight locomotive. J Traffic Transp Eng. 2012;12(3):37–43.
[14] Yao Y, Zhang XX, Zhang HJ, Luo S. The stability mechanism and its application of heavy haul couplers with arc surface contact. Veh Syst Dyn. 2013;51(9):1324–1341. doi:10.1080/00423114.2013.801500
[15] Ma WH, Luo SH, Song RR. Coupler dynamic performance analysis of heavy haul locomotive. Veh Syst Dyn. 2012;50:1435–1452.
[16] Zhai WM. Vehicl-track coupling dynamics. 3rd ed. Beijing: Science Press, ISBN 978-7-03-018326-2; 2007 (in Chinese).